Journal of the Serbian Chemical Society
JSCS@tmf.bg.ac.rs • www.shd.org.rs/JSCS
J. Serb. Chem. Soc. *87* (11) 1273–1284 (2022)
JSCS–5593
Original scientific paper
Published 16 September 2022

Binding of *β*-casein with fluvastatin and pitavastatin

HAMID DEZHAMPANAH* and OMIDEH RAJABI MIANDEHI

Department of Chemistry, Faculty of Science, University of Guilan, P.O.B. 1914, Rasht 0098, Iran

(Received 6 June, revised 30 July, accepted 9 August 2022)

Abstract: In this work, the binding interaction of fluvastatin (FLU) and pit-avastatin (PIT) with bovine *β*-casein (*β*-CN) were performed under physiological conditions (pH 7.2) by fluorescence emission spectroscopy, synchronous fluorescence spectroscopy, Fourier transform infrared spectroscopy (FTIR) and molecular docking methods. Due to the formation of FLU-*β*-CN and PIT-*β*-CN complexes, the intrinsic fluorescence of *β*-CN was quenched. The number of bound FLU and PIT per protein molecule (*n*) were about 1, also the binding constant of FLU-*β*-CN and PIT-*β*-CN complexes were 7.96×10^4 and 3.44×10^4 M^{-1} at 298 K, respectively. This result suggests that the binding affinity of FLU to *β*-CN was higher than that for PIT. Molecular modelling showed different binding sites for FLU and PIT on *β*-CN. All these experimental results suggest that *β*-CN can be used as a carrier protein which delivers FLU and PIT based drugs to target molecules.

Keywords: milk protein; statin; molecular modelling; spectroscopy.

INTRODUCTION

Statins are a group of medicines that can help lower the level of low-density lipoprotein (LDL) cholesterol in blood. They act as potentially competitive inhibitors of 3-hydroxy-3-methylglutaryl-coenzyme A (HMG-CoA) reductase, which catalyzes the rate-limiting phase of the cholesterol biosynthesis cascade.[1,2] Statins can be classified as natural statins and synthetic statins. Lovastatin is a fermentation-derived statin whereas simvastatin is a semi-synthetic statin synthesized from lovastatin either by synthetic or enzymatic biotransformation routes. There are several synthetic statins are available at the market, such as cerivastatin, atorvastatin, fluvastatin, pitavastatin and rosuvastatin, which are more effective than fermentation-derived statins. FLU (Fig. S-1 of the Supplementary material to this paper) is an HMG-CoA reductase inhibitor that is used to lower lipid levels.[4] It effectively lowers the serum LDL-cholesterol level and reduces

* Corresponding author. E-mail: h.dpanah@guilan.ac.ir
https://doi.org/10.2298/JSC220606067D

the risk of the development of atherosclerosis. Recent studies have reported that FLU is a new therapeutic agent for the prevention and the treatment of breast cancer,[5] and it has also been shown that some statins, including FLU, may have a potential effect in the treatment of COVID-19.[6] PIT (Fig. S-1) is also a unique lipophilic statin with a strong effect in lowering total plasma cholesterol and triglycerides. The unique lipid and non-lipid effects of PIT make this molecule a particularly interesting option for the management of different human diseases.[7]

Milk is a unique source of nutrients and is widely recognized by consumers as a source of compounds beneficial to growth and health in children and adults.[8] Milk proteins are classified into two distinct groups, casein, and whey or serum protein. Caseins as a functional food have a great variety and play an essential role in the development of new food products. Casein is one of the two main components of milk protein, making up about 40 % of the protein in human milk and approximately between 78 and 86 % of the protein in house mice, cow, sheep, goat and buffalo milk.[9] Casein is found in local milk as supramolecular aggregates called casein micelles, which are between 50 to 600 nm in diameter.[10] They occur as micelles made up of four main components: α_{s1}-, α_{s2}-, β- and κ-casein at a mole ratio of about 4:1:4:1. About 38 % of this structure is formed by β-CN, which contains 209 amino acids, has a monomeric molecular mass of approximately 24 kDa. It is more hydrophobic than that in α- and κ-casein and contains one tryptophan (Trp) residu.[11,12] Bovine β-casein is an extremely amphiphilic protein consisting of a hydrophilic N-terminal segment with a hydrophobic C-terminal segment and a group consisting of five phosphoryl residues.[12]

The aim of this work was to investigate the interaction of bovine β-CN with FLU and PIT. The overall binding constant of FLU and PIT to β-CN were calculated at 298 K and the effect of FLU and PIT on the conformation of β-CN was evaluated. For this purpose, molecular docking experiments and multi-spectroscopic measurements were conducted, which may extend the versatile use of β-CN as a transporter for the delivery of therapeutic, or as solubilizing agents in food applications. We also compared the binding affinity of the β-CN fraction and the probable binding sites of FLU and PIT in the β-CN fraction by both experiments and molecular modelling studies.

EXPERIMENTAL

Fluorescence spectroscopy

The fluorescence measurements were performed using Varian Cary Eclipse spectrofluorometer containing a 1.0 cm quartz cuvette, with an optical pathway of 1 cm, from 290 to 440 nm. The excitation wavelength was set at 280 nm, and the excitation and emission slits were adjusted at 5 nm. For the preparation of FLU and PIT with β-CN complexes, a 1 mM stock solution of FLU and PIT in ethanol and methanol were prepared, respectively. The entrapment of each FLU and PIT in β-CN molar ratios was performed by adding different volumes of FLU and PIT solutions to a β-CN solution with continuous stirring. In this work,

all fluorescence intensities were corrected for inner filter effect, due to the UV absorption of FLU and PIT with β-CN and the mean values were calculated according to:

$$F_c = F_m e^{((A_1 + A_2)/2)} \quad (1)$$

where A_1 and A_2 are the absorbance of FLU and PIT at excitation and emission wavelengths, respectively. F_c and F_m are the corrected and the experimentally measured fluorescence intensities, respectively.

Synchronous fluorescence spectroscopy experiments

Spectra of β-CN solution in the absence and presence of FLU and PIT were measured at 298 K. The values of wavelength intervals which is the difference between the emission wavelength (λ_{em}), and the excitation wavelength (λ_{ex}), was set at 15 and 60 nm, respectively. The scanning wavelength range was set at 200–400 nm. The concentrations of FLU varied from 0 to 18 μM, PIT varied from 0 to 23 μM and the concentration of β-CN was 1 mM.

FT-IR spectroscopic measurements

FT-IR measurements were performed at room temperature by an ALPHA FT-IR spectrometer (Bruker) optics using a KBr pellet in the range of 4000–400 cm^{-1}. FLU and PIT solutions were added dropwise to the β-CN solution with continuous stirring to form a homogeneous solution. The FLU and PIT concentrations were 0, 0.25, and 0.5 mM with a fixed β-CN solution of 0.25 mM.[19] Then the solutions were freeze-dried in Christ Alpha 1-2 LD freeze dryer at –40 °C for 4 h. The pellets were prepared by mixing the freeze-dried sample with KBr and pressed under vacuum at pressure for three minutes.[20]

Molecular modelling and docking

The 3D structure of FLU and PIT were made using Gauss view 5.0. The geometry of FLU and PIT were optimized by the density functional theory (DFT) (B3LYP/6-31G*(d.p)) using Gaussian 03. Milk β-CN structure was made according to Swiss-Model, protein models were first modified by adding all hydrogen atoms and removing water molecules based on the builder module of AutoDock. The macromolecules were rigidly maintained, while all the torsional bonds of the ligands were released for rotation. AutoDock Vina was used to simulate the binding conformation of β-CN with FLU and PIT using the Lamarckian genetic algorithm.[21] AutoDock and Ligplus+ tools were used to get the best molecular docking results. The lowest energy docked structure was obtained using a grid map with 70×70×70 points and a grid point spacing of 0.1 nm and the maps were centered on this new docking location. The Lamarckian genetic algorithm was employed with the following parameters: 10 docking runs with 25,000,000 energy evaluations for each run. The conformer with the lowest binding energy was used for further analyses.[22]

RESULTS AND DISCUSSION

Fluorescence quenching of β-*CN*

When the binding interaction of proteins and drug molecules occurs, fluorescence spectroscopy analysis can be used to obtain the important data of binding constants and the number of binding sites. When excited at 280 nm, amino acids with phenyl rings such as tryptophan (Trp), tyrosine (Tyr) and phenylalanine (Phe) cause the intrinsic fluorescence of the protein.[25] The β-CN contains one tryptophan Trp-143 with an intrinsic fluorescence, when other molecules interact with casein, tryptophan fluorescent can change based on the effect of such inter-

action on protein conformation. The decrease of fluorescence intensity of β-CN has been monitored at 346 nm for β-CN with FLU and PIT in Fig 1a and b. The fluorescence spectra of all β-CN solutions in the absence and presence of FLU and PIT were shown in Fig. 1a and b. The results revealed that the fluorescence intensities of β-CN decreased progressively with the successive increases of FLU and PIT concentrations, suggesting that there were changes in the microenvironment surrounding Trp residue due to the binding interaction of FLU and PIT with β-CN. The decrease in the fluorescence intensity with increasing FLU and PIT concentrations also indicated the energy transfer between the fluorophore in β-CN with FLU and PIT. Also, we observed the blue shift of maximum emission wavelength (λ_{em}) about 1 and 3 nm for β-CN with FLU and PIT, respectively, further indicating that the microenvironment surrounding Trp residue was relatively more hydrophobic upon FLU and PIT binding. The fluorescence quenching of protein can be classified into three. The static quenching is caused by producing a ground-state complex of protein and quenchers. Whereas, dynamic quenching is caused by protein and quencher conflicts, and coupled dynamic and static quenching caused both conflict and complexity.[26] Both static and dynamic processes can be defined the Stern–Volmer Equation as follows:[27]

$$\frac{F_0}{F} = 1 + K_{SV}C_Q = 1 + k_q\tau_0 C_Q \quad (2)$$

where F_0 and F are fluorescence intensities in the absence and presence of quencher, C_Q is quencher concentration and K_{SV} is Stern–Volmer constant, which can be calculated using the linear slope of plot of F_0/F *vs.* C_Q (of FLU or PIT) are shown in Fig 1a and 1b.[29] also (inset), respectively. k_q is the bimolecular quenching rate constant and τ_0 is the lifetime of the fluorophore in

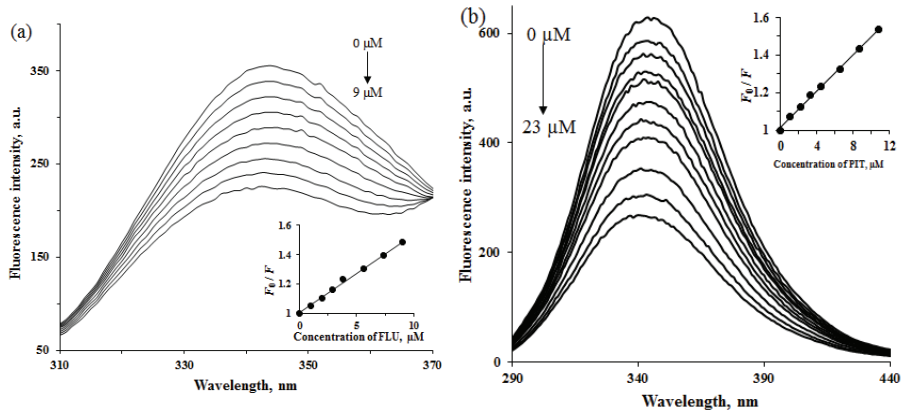

Fig. 1. Fluorescence spectra of β-CN (10 μM) induced by the different concentration of FLU and PIT at 298 K, FLU-β-CN (a) and PIT-β-CN (b). Inset: Stern–Volmer plots for the quenching of β-CN (10 μM) induced by the different concentration of FLU and PIT.

the absence of quencher: 3.30 ns for β-CN.[28] According to the formula, the Stern–Volmer (S–V) curve of β-CN interacting with FLU and PIT were in a linear relationship (Fig. 1).[29] Also, with the use of the equation we observed that k_q for complex FLU–β-CN and PIT–β-CN is 1.6×10^{13} and 1.45×10^{13} M^{-1} s^{-1}, respectively, which is greater than the maximum diffusion collision quenching rate constant (2.0×10^{10} M^{-1} s^{-1}). These results indicate that the static quenching effect exists in the system of FLU and PIT with β-CN.[30,31]

For the quenching process of β-CN, the binding constant (K_b) of a complex of FLU and PIT with β-CN can be determined by (Fig. S-2 of the Supplementary material):[27]

$$\log\frac{F_0 - F}{F} = \log K_b + n\log C_Q \quad (3)$$

which is equal 7.96×10^4 and 3.44×10^4 M^{-1} at 298 K, as shown in Table I, respectively. Also, the number of binding sites (n) obtained for both complexes is about 1. An n value of approximately equal to 1 illustrated that there was only a single binding site in the binding of FLU and PIT with β-CN as shown in Table I.[27]

TABLE I. The quenching constants of β-casein by FLU and PIT

Complex	K_{SV} / mM^{-1}	R^2	n	K_b / mM^{-1}	R^2
FLU–β-casein	0.537±0.001	0.9967	1.02±0.02	0.796	0.9962
PIT–β-casein	0.481±0.012	0.9973	0.96±0.02	0.344	0.9939

Energy transfer from β-*CN to FLU and PIT*

Förster resonance energy transfer (FRET) is a mechanism describing energy transfer between two light-sensitive molecules. A donor chromophore, initially in its electronic excited state, can transfer energy to an acceptor chromophore through nonradiative dipole-dipole coupling.[32] Eq. (4) is used to estimate the spatial distances between the donor (protein) and the receptor (ligand) in which the efficiency of this energy transfer (E) is inversely proportional to the sixth power of the distance between the donor and the acceptor:[33]

$$E = 1 - \frac{F}{F_0} = \frac{R_0^6}{R_0^6 + r^6} \quad (4)$$

where F_0 and F are the fluorescence intensity of donor in the absence and presence of acceptor, respectively. r is the distance between the donor and acceptor, and R_0 is the Förster critical distance when the efficiency (E) is 50 %, which can be computed as:[34]

$$R_0{}^6 = 8.8\times10^{-4}K^2N^{-4}\phi \quad (5)$$

where $K = 2/3$ is a factor describing the relative orientation of the transition dipoles of the donor and acceptor, $N = 1.53$ is the average refractive index of the

environment in the wavelength range where the spectral overlap is significant, φ = 1.49 for casein, which is the fluorescence quantum yield of the donor in the absence of acceptor.[20] Overlap integral J expresses the extent of overlap between the normalized fluorescence emission spectrum of donor and absorption spectrum of the acceptor, which is measured by:[34]

$$J = \frac{\sum F(\lambda)\varepsilon(\lambda)\lambda^4\Delta\lambda}{\sum F(\lambda)\Delta\lambda} \quad (6)$$

Where $F(\lambda)$ is the fluorescence intensity of the fluorescent donor at a wavelength of λ, and $\varepsilon(\lambda)$ is the molar absorption coefficient of the acceptor at a wavelength of λ. (Fig. S-3 of the Supplementary material) show the spectral overlap of fluorescence emission of β-CN and absorption spectrum of FLU and PIT, respectively. According to the above equations, R_0 = 1.52 nm, r = 1.72 nm, and J = = 4.55×10^{-16} cm^3 L mol^{-1} for β-CN-FLU and R_0 = 2.05 nm, r = 2.23 nm, and J = 2.74×10^{-15} cm^3 L mol^{-1} for β-CN-PIT were calculated. As the distance between casein (donor) and FLU or PIT (acceptor) was less than 8 nm with the rule $0.5R_0 < r < 1.5R_0$, suggesting that the energy transfer from β-CN to FLU and PIT occurs with high probability and distance, obtained by Förster resonance energy transfer with higher accuracy.[32] The short distance values also suggested strong interaction between FLU and PIT with residues of β-CN. In addition, the value of r was larger than the respective critical distance (R_0), indicating that the fluorescence quenching mechanism of β-CN is inducted by is static quenching.[32,35]

Synchronous fluorescence spectroscopy

Simultaneous fluorescence spectroscopy is often used to consider changes in the microenvironment of Tyr ($\Delta\lambda$ = 15 nm) and Trp ($\Delta\lambda$ = 60 nm) fluorophores as well as to study changes in protein structure. The shift of maximum emission wavelength (λ_{em}) indicates the change in the polarity of the microenvironment surrounding Tyr or Trp residues. The red shift of λ_{em} indicates the decrease in the hydrophobicity surrounding Tyr or Trp residue and also the increase in the stretching extent of the peptide chain. In contrast, a change in blue λ_{em} indicates an increase in hydrophobicity around the residual Tyr or Trp and a fold state for the macromolecule. The synchronous fluorescence spectra of β-CN with the addition of FLU and PIT were shown in Figs. S-4 and S-5 of the Supplementary material. The results revealed that the fluorescence quenching effect of FLU and PIT on Trp was higher than on Tyr in β-CN. These results indicate that FLU and PIT are located closer to Trp than to Tyr when binding to β-CN. In addition, in Fig.S-4, the weak red shift (1 nm) of the λ_{em} of Tyr residue was observed (1 nm) with $\Delta\lambda_{em}$ setting at 15 nm, while the blue shift of the λ_{em} of Trp residue was observed (3 nm) with $\Delta\lambda_{em}$ setting at 60 nm. The adding of the concentration of

FLU, indicated that the hydrophobic characteristics surrounding Tyr residue and the folding state of β-CN slightly decreased as the hydrophobic characteristics surrounding Trp residues and the folding state of β-CN increased. Also, in Fig. S-5 the red shift (2 and 3 nm) of the λ_{em} of Tyr and Trp residues were observed with $\Delta\lambda_{em}$ setting at 15 and 60 nm respectively, with adding the concentration of PIT, indicating that the hydrophobic characteristics surrounding Tyr and Trp residues and the folding state of β-CN decreased. So, it resulted in the β-CN composition change after binding to FLU and PIT.

FTIR spectroscopy

IR spectroscopy has been used as a powerful method to study the secondary structure of proteins and their dynamics.[36] Because the IR spectra of proteins exhibit several so-called amide bands, which represent different vibrations of the peptide moiety, and there was no major spectral shifting, the protein amide I peak position which occurred in the region between 1600 and 1700 cm^{-1} (principally C=O stretch) and the amide II band 1500–1600 cm^{-1} (C–N stretch coupled with N–H bending mode) have been widely used as typical and both are related to the secondary structure of the protein.[37] The amide I bond is useful in studying the secondary structure because the amide I bond is more sensitive to changes in the secondary structure of the protein than amide II. Here, the amide I absorption peak of β-CN shifted from the wavenumber, and the intensity of β-CN was changed for C=O stretch (amide I band) at 1646 cm^{-1} and C–N stretching participant with N–H bending modes (amide II band) at 1536 cm^{-1}, due to the hydrophilic contacts of FLU and PIT with β-CN. To further investigate the manner of FLU and PIT interaction, the difference spectra for (protein solution + drug solution) – protein solution were obtained. The intensity variations of amide I and amide II bands were monitored upon FLU and PIT complexation, and results are shown in Figs. S-6 and S-7 of the Supplementary material.

In Fig. S-6a, at low FLU concentration (0.25 mM), a decrease in the intensity of β-CN was observed. The spectral shifting was observed for the protein amid II bands at 1534 cm^{-1} for β-CN. As FLU concentration increased to 0.5 mM, a decrease of intensity was observed for amide I and amide II bands at 1644 and 1533 cm^{-1} for FLU β-CN. Also, in Fig. S-6b, at low PIT concentration (0.25 mM), a decrease in the intensity of β-CN was observed. The spectral shifting was observed for the protein amid the I band at 1649 cm^{-1} and amide II at 1514 cm^{-1} for β-CN. While as PIT concentration increased to 0.5 mM, a rise of intensity was observed for amide I and amide II bands at 1649 and 1512 cm^{-1}, respectively, for β-CN-PIT. The hydrophobic contacts in the complex of FLU and PIT with β-CN were analyzed from spectral changes of the β-CN CH_2 antisymmetric and symmetric stretching vibrations, in the region of 2800–3000 cm^{-1}. The CH_2 bands of free β-CN at 2872, 2928 and 2957 cm^{-1} shifted to 2872, 2929 and 2956

cm^{-1} and to 2869, 2928, 2955 cm^{-1} with the addition FLU; it that was shown in Fig. S-7a. With the addition PIT it shifted to 2853, 2928 and 2963 cm^{-1} and to 2855, 2925 and 2952 cm^{-1}, which was observed in Fig. S-7b. These changes in the infrared spectra of *β*-CN confirmed the change in the conformation of *β*-CN by the addition of FLU and PIT.[20] Similar results are obtained from the fluorescence spectroscopy data.

The data in the 1600–1700 cm^{-1} region were further analyzed to quantify the secondary structure content of *β*-CN using the Fourier self-deconvolution and second derivative technique. They were estimated as shown in Fig. S-8a and Table S-I of the Supplementary material; the free *β*-CN has 28.13 % *α*-helix (1646 cm^{-1}), 17.67 % *β*-sheet (1619–1624 cm^{-1}), 22.04 % turn structure (1657 cm^{-1}), 7.13 % *β*-antiparallel (1666 cm^{-1}) and random coil 24.43 % (1635 cm^{-1}). Upon FLU interaction, a decrease of the *β*-turn and *β*-anti-parallel occurred for FLU–*β*-CN complex, while an increase of *α*-helix, *β*-sheet and random coil were observed in Fig. S-8b and Table S-I. Also, a decrease of the *α*-helix, random coil, *β*-turn and *β*-anti parallel and increase of *β*-sheet were observed for PIT–*β*-CN complex, Fig, S-8c and Table S-I. The results revealed that the change in the conformational of *β*-CN was due to the binding *β*-CN with FLU and PIT.

Docking studies

In recent years, molecular docking has been used as an important technique for ligand-protein studies that provides more detailed information about the interaction between ligands and proteins.[38] Based on the experiment data, computational docking studies were made to understand the binding site location and the best conformation for binding of FLU and PIT to *β*-CN using binding free energy evaluation. Using intermolecular energy, internal energy and torsional free energy, the energies estimated by AutoDock can be described. Among these calculated energies by AutoDock, the first two provide the docking energy while the sum of the first and third items account for the binding energy.[18] The dominating conformation of the binding complex of *β*-CN with FLU and PIT, which was the lowest binding free energy, was shown in Fig. 2 and Table S-II. In Fig. 3a (FLU––*β*-CN complex), FLU molecule is surrounded by Ile-41 with forming one hydrogen bond with a length of 3.25 Å (FLU-amino acid) and Leu-6, Leu-9, Val-10, Ala-13, Leu-14, Arg-40, Leu-60, Lys-63, Ile-64 and Phe-67 by hydrophobic interaction and free binding energy of –27.58 kJ mol^{-1} as shown in Table S-II. Fig. 3b (PIT–*β*-CN complex), shows that the PIT molecule is surrounded by His--160, Lys-184, Pro-187 and Pro-196 forming four hydrogen bonds with lengths of 3.06, 2.91, 3.14 and 2.96 Å, and Met-159, His-163, Gln-164, Pro-165, Leu--166, Ser-183 and Pro-189 by hydrophobic interaction and free binding energy of –27.17 kJ mol^{-1}. The binding energy shows the FLU–*β*-CN is more stable than PIT–*β*-CN complex. It can be seen from Fig. 3a and b that the distance between

donor and acceptor atoms is from 2.6 to 3.5, which can play an important role in the binding of FLU and PIT to β-CN. So, it can be concluded that the interaction between β-CN and FLU and PIT is mainly a hydrophobic interaction and a hydrogen bonding interaction in nature. The docking results reveal that the interactions between FLU and PIT and β-CN are in good agreement with experimental results.

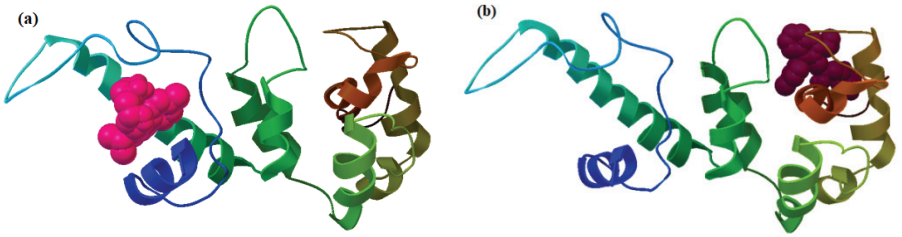

Fig. 2. Structures of complex with lowest binding free energy β-CN+FLU (a) and β-CN+PIT (b).

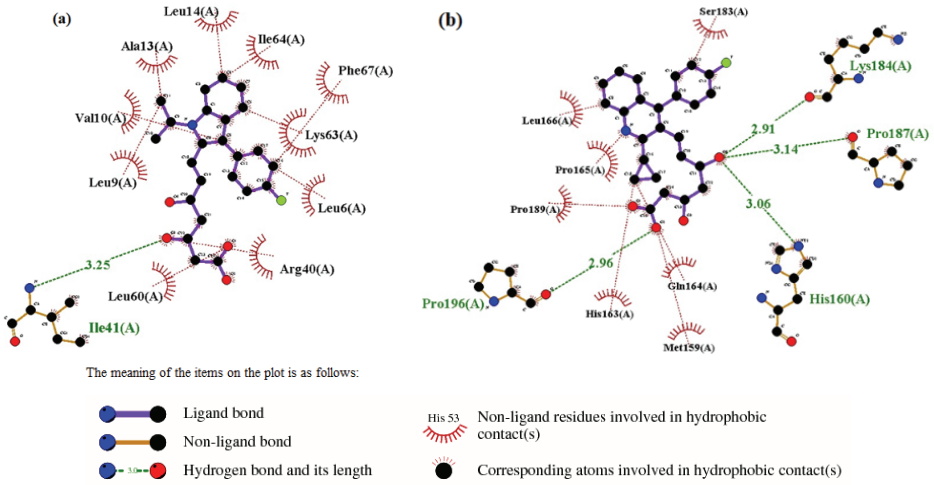

Fig. 3. Best conformations for β-CN docked to: a) FLU and b) PIT.

CONCLUSION

In this work, the binding interactions of FLU–β-CN and PIT–β-CN were studied by multi-spectroscopic and molecular docking methods. The results suggested that the intrinsic fluorescence of β-CN can be quenched by FLU and PIT through the static quenching mechanism. The number of binding sites (n) for FLU and PIT was found to be about 1. The binding constants, at 298 K, were determined according to a modified Stern–Volmer equation as 7.96×10^4 and 3.44×10^4 M^{-1} for FLU–β-CN and PIT–β-CN, respectively. The binding distance

(r_0) between FLU and PIT and Trp-residue of β-CN were calculated as 1.72 and 2.23 nm, respectively, according to Förster's non-radiative energy transfer theory.

SUPPLEMENTARY MATERIAL

Additional data and information are available electronically at the pages of journal website: https://www.shd-pub.org.rs/index.php/JSCS/article/view/11905, or from the corresponding author on request.

ИЗВОД

ВЕЗИВАЊЕ β-КАЗЕИНА ЗА ФЛУВАСТАТИН И ПИТАВАСТАТИН

HAMID DEZHAMPANAH и OMIDEH RAJABI MIANDEHI

Department of Chemistry, Faculty of Science, University of Guilan, P.O.B. 1914, Rasht 0098, Iran

У овом раду су проучене везивне интеракције флувастатина (FLU) и питавастатина (PIT) са говеђим β-казеином (β-CN) у физиолошким условима (pH 7,2) помоћу флуоресцентне емисионе спектроскопије, спектроскопије синхроне флуоресценције, FT инфрацрвене спектроскопије (FTIR) и методама молекулског докинга. Због формирања FLU–β-CN и PIT–β-CN комплекса, својствена флуоресценција β-CN била је пригушена. Број везаних FLU и PIT по молекулу протеина (n) био је око 1, а константе везивања FLU–β-CN и PIT–β-CN комплекса су биле $7{,}96\times10^4$, односно $3{,}44\times10^4$ M^{-1} на 298 K. Ови резултати сугеришу да је везивни афинитет FLU према β-CN већи од везивног афинитета PIT. Молекулско моделовање показује различита везивна места за FLU и PIT на β-CN. Сви ови експериментални резултати сугеришу да β-CN може деловати као носећи протеин за лекове FLU и PIT при њиховом достављању на циљне молекуле.

(Примљено. 6. јуна, ревидирано 30. јула,прихваћено 9. августа 2022)

REFERENCES

1. M. Gupta, R. Sharma, A. Kumar, *Pharm. Exp. Med*. **19** (2019) 259 (https://doi.org/10.1007/s13596-019-00393-x)
2. J. H. Shi, Q. Wang, D. Q. Pan, T. T. Liu, M. Jiang. *J. Biomol. Struct. Dyn*. **35** (2017) 1529 (https://doi.org/10.1080/07391102.2016.1188416)
3. A. L. Toppo, M. Yadav, S. Dhagat, S. Ayothiraman, J. S. Eswari, *Ind. J. Biochem. Biophys*. **58** (2021) 127
4. M. S. Khan, *Ann. Romanian Soc. Cell Biol*. **25** (2021) 6244
5. J. S. Yu, D. H. Shin, J. Kim, *Pharmaceutics* **12** (2020) 1133 (https://doi.org/10.3390/pharmaceutics12121133)
6. Ž. Reiner, M. Hatamipour, M. Banach, M. Pirro, K. Al-Rasadi, *Arch. Med. Sci*. **16** (2020) 490 (https://dx.doi.org/10.5114%2Faoms.2020.94655)
7. A. Sahebkar, N. Kiaie, A. M. Gorabi, M. R. Mannarino, V. Bainaconi, T. Jamialahmadi, M. Pirro, M. Banach, Prog. *Lipid Res*. **84** (2021) 101127 (https://doi.org/10.1016/j.plipres.2021.101127)
8. S. Rahimi Yazdi, M. Corredig, *Food Chem*. **132** (2012) 1143 (https://doi.org/10.1016/j.foodchem.2011.11.019)
9. K. L. Field, B. A. Kimball, J. A. Mennella, G. K. Beauchamp, A. A. Bachmanov, *Physiol. Behav*. **93** (2008) 189 (https://doi.org/10.1016/j.physbeh.2007.08.010)
10. Z. Allahdad, M. Varidi, R. Zadmard, A. Akbar, *Food Chem*. **255** (2018) 187 (https://doi.org/10.1016/j.foodchem.2018.01.143)

11. H. E. Indyk, B. D. Gill, J. E. Wood, S. Chetikam, T. Kobayashi, *J. Food Compos. Anal.* **101** (2021) 103946 (https://doi.org/10.1016/j.jfca.2021.103946)
12. M. Li, R. Kembaren, Y. Ni, J.M. Kleijn, *Food Chem*. **352** (2021) (https://doi.org/10.1016/j.foodchem.2021.129400)
13. N. Sarreshtehdari, F.S. Mohseni-Shahri, F. Moeinpour, *Luminescence* **36** (2021) 360 (https://doi.org/10.1002/bio.3951)
14. I. Portnaya, U. Cogan, Y. D. Livney, O. Ramon, K. Shimoni, M. Rosenberg, D. Danino, *Food Chem*. **54** (2006) 5555 (https://doi.org/10.1021/jf060119c)
15. J. Kaur, L. Katopo, A. Hung, J. Ashton, S. Kasapis, *Food Chem*. **252** (2018) 163 (https://doi.org/10.1016/j.foodchem.2018.01.091)
16. D. C. Thorn, S. Meehan, M. Sunde, A. Rekas, S. L. Gras, C. E. MacPhee, C. M. Dobson, M. R. Wilson, J. A. Carver, *Biochemistry* **44** (2005) 17027 (https://doi.org/10.1021/bi051352r)
17. L. Condict, J. Kaur, A. Hung, J. Ashton, S. Kasapis, *Food Hydrocoll*. **89** (2019) 351 (https://doi.org/10.1016/j.foodhyd.2018.10.055)
18. F. Mehranfar, A. K. Bordbar, H. Parastar, *J. Photochem. Photobiol., B* **127** (2013) 100 (https://doi.org/10.1016/j.jphotobiol.2013.07.019)
19. I. Hasni, P. Bourassa, S. Hamdani, G. Samson, R. Carpentier, H. A. Tajmir-Riahi, *Food Chem*. **126** (2011) 630 (https://doi.org/10.1016/j.foodchem.2010.11.087)
20. H. Dezhampanah, M. Esmaili, A. Khorshidi, *J. Mol. Struct*. **1136** (2017) 50 (https://doi.org/10.1016/j.molstruc.2017.01.065)
21. T. Liao, Y. Zhang, X. Huang, Z. Jiang, X. Tuo, *Spectrochim. Acta, A* **246** (2021) 119000 (https://doi.org/10.1016/j.saa.2020.119000)
22. F. Kong, J. Tian, M. Yang, Y. Zheng, X. Cao, X. Yue, *Spectrochim. Acta A* **243** (2020) (https://doi.org/10.1016/j.saa.2020.118824)
23. B. Li, R. Fu, H. Tan, Y. Zhang, W. Teng, Z. Li, J. Tian, *Spectrochim. Acta, A* **259** (2021) 119910 (https://doi.org/10.1016/j.saa.2021.119910)
24. Q. Wang, C. R. Huang, M. Jiang, Y. Y. Zhu, J. Wang, J. Chen, J. H. Shi, *Spectrochim. Acta, A* **156** (2016) 155 (https://doi.org/10.1016/j.saa.2015.12.003)
25. Z. Yin, X. Qie, M. Zeng, Z. Wang, F. Qin, J. Chen, W. Li, Z. He, *Food Hydrocoll*. **123** (2022) 107177 (https://doi.org/10.1016/j.foodhyd.2021.107177)
26. F. Azarakhsh, A. Divsalar, A. A. Saboury, A. Eidi, *J. Mol. Liq*. **333** (2021) 115999 (https://doi.org/10.1016/j.molliq.2021.115999)
27. G. Ma, C. Tang, X. Sun, J. Zhang, *Food Hydrocoll*. **113** (2021) 106485 (https://doi.org/10.1016/j.foodhyd.2020.106485)
28. 28. A. Chakraborty, S. Basak, *J. Photochem. Photobiol., B* **87** (2007) 191 (https://doi.org/10.1016/j.jphotobiol.2007.04.004)
29. H. Dezhampanah, R. Firouzi, Z. Moradi Shoeili, R. Binazir, *J. Mol. Struct*. **1205** (2020) 127557 (https://doi.org/10.1016/j.molstruc.2019.127557)
30. K. Yang, C. Zhou, C. Liao, J. Sun, Y. Wang, R. Guan, J. Neng, P. Sun, *LWT* **144** (2021) 111225 (https://doi.org/10.1016/j.lwt.2021.111225)
31. M. Ariyaeifar, H. Amiri Rudbari, M. Sahihi, Z. Kazemi, A. A. Kajani, H. Zali-Boeini, N. Kordestani, G. Bruno, S. Gharaghani, *J. Mol. Struct*. **1161** (2018) 497 (https://doi.org/10.1016/j.molstruc.2018.02.042)
32. J. H. Shi, J. Wang, Y. Y. Zhu, J. Chen, *J. Lumin*. **145** (2014) 643 (https://doi.org/10.1016/j.jlumin.2013.08.042)
33. J. Hua Shi, D. Qi Pan, X. Xiou Wang, T. T. Liu, M. Jiang, Q. Wang, *J. Photochem. Photobiol., B* **162** (2016) 14–23 (https://doi.org/10.1016/j.jphotobiol.2016.06.025)

34. B. Hemmateenejad, M. Shamsipur, F. Samari, T. Khayamian, *J. Pharm. Biomed. Anal.* **67**–**68** (2012) 201 (https://doi.org/10.1016/j.jpba.2012.04.012)
35. H. Bi, L. Tang, X. Gao, J. Jia, H. Lv, *J. Lumin*. **178** (2016) 72 (https://doi.org/10.1016/j.jlumin.2016.05.048)
36. S. Gong, C. Yang, J. Zhang, Y. Yu, X. Gu, W. Li, Z. Wang, *Food Hydrocoll.* **111** (2021) 106223 (https://doi.org/10.1016/j.foodhyd.2020.106223)
37. P. Bourassa, L. Bekale, H. A. Tajmir-Riahi, *J. Biol. Macromol*. **70** (2014) 156 (https://doi.org/10.1016/j.ijbiomac.2014.06.038)
38. S. K. Pawar, S. Jaldappagari, *J. Pharm. Anal*. **9** (2019) 274 (https://doi.org/10.1016/j.jpha.2019.03.007).